Development of Fibre Optic Broadband Sources at 1 μm region for Optical Coherence Tomography

Irina Trifanov, Martin O. Berendt, José R. Salcedo, Adrian Gh. Podoleanu[(a)], António B. Lobo Ribeiro

Multiwave Photonics S.A., R. Eng. Frederico Ulrich 2650, 4470-605 Moreira da Maia, Portugal
(a) Applied Optics Group, School of Physical Sciences, University of Kent, Canterbury, Kent CT2 7NR, UK

ABSTRACT

Recent developments on broadband optical sources emitting at 1050 nm wavelength for medical applications, in particular optical coherence tomography (OCT), have revealed enhanced depth penetration into the choroid, reduced scattering losses and improved image performances in eyes with turbid media, when compared to the most commercial used semiconductor optical source technology at 820 nm. In this paper, we present our study of fibre optic broadband sources (BBS) at 1 micron region, based on the amplified spontaneous emission (ASE) from rare-earth doped silica fibres for the integration into OCT systems. The target specifications for this type of sources are: 1050 nm central emission wavelength, with spectral width of ~70 nm, tens of miliwatts of output power and smoothly shaped output spectra. Several combinations of rare-earth doped optical fibres integrated into different fibre optic configurations have been tested. Optical bandwidth optimization and spectral shaping using different fibre optic techniques are presented and their autocorrelation function compared.

Keywords: fibre optic broadband sources, optical coherence tomography.

1. INTRODUCTION AND MOTIVATION

Optical Coherence Tomography (OCT) has already been established as a state-of-the-art imaging technique [1] for a wide range of applications in biomedicine and industry. Among these, more than 50% are in ophthalmology, because OCT addresses a fundamental limitation of confocal microscopy. Its non-invasive, non-contact, *in-vivo* and real-time imaging capabilities makes OCT ideally suited to imaging solutions to replace biopsy and histopathology.

The most commonly used light sources in commercial OCT systems have been superluminescent diodes (SLDs) centred either at 800 nm or 1300 nm wavelength. To meet the demands of the latest generation of OCT systems with video scan rates and ultrahigh resolutions, Kerr–lens mode-locked Ti:sapphire lasers had been employed in laboratory tests. Since then, the main activity has been the development of a variety of optical sources primarily based on supercontinuum generation in various forms of optical fibres. Primary objectives for these OCT systems have been to push the axial resolution as high as possible, to cover the main spectral range imaging windows (visible and mid-IR regions), and to reduce the complexity, cost and size of such optical sources.

Commercially available retinal ophthalmic OCT systems operate at ~ 820 nm because of the lowest cumulated absorption of the eye tissue at this wavelength. Although the majority of retina imaging reports refers to this band, and ultrahigh resolution has also been demonstrated in this wavelength region for resolving intra-retinal layers [2], it has limited depth penetration beyond retinal pigment epithelium (RPE). For imaging features beyond the RPE, longer wavelengths are more suitable [3]. This relates to the fact that the absorption and scattering properties of melanin (the main chromophore in the RPE) tend to decrease with increasing wavelength. Water absorption, on the other hand,

1st Canterbury Workshop on Optical Coherence Tomography and Adaptive Optics
edited by Adrian Podoleanu, Proc. of SPIE Vol. 7139, 713906 · © 2008 SPIE
CCC code: 0277-786X/08/$18 · doi: 10.1117/12.815347

represents a more critical limitation especially when imaging biological sample, because of their high content (~90%) of water. There is, however, a spectral window restricted to a wavelength span of 100 nm (from 1 - 1.1 μm) where the water absorption spectrum exhibits a minimum value. Moreover, the optical power loss due to increased water absorption compared to 800 nm is compensated by the fact that the permissible corneal exposure for longer wavelengths also increases, according to ANSI standards [4]. An additional advantage of optical imaging at 1 μm wavelengths region is the zero dispersion point of water, which eliminates the depth dependent broadening of axial resolution over reasonable depth penetration.

Recent development of broadband light sources centred at 1050 nm based on amplified spontaneous emission (ASE) from rare-earth doped fibres made possible the development of OCT systems in this band. Moreover, optical frequency domain imaging using swept laser sources is an emerging second-generation method for optical coherence tomography. The most successful configurations used at 1 micron are cavity tuned lasers based on semiconductor amplifiers (SOAs), either with fibre Fabry–Perot tuning filters [5, 6] or polygon scanning filters [7] driven at scanning speeds of several tens and hundreds of kHz. Both modalities have proven successful for 3D in vivo retinal imaging with enhanced performance and penetration [8, 9]. It is predicted that this imaging modality could become a successful alternative to imaging at 800 nm in early assessments, staging and therapeutic monitoring of retinal diseases.
So far, little effort has been put into building commercial OCT imaging systems using reliable broadband sources around ~ 1 μm. *In-vitro* experimental studies have demonstrated ultrahigh axial resolutions of about 1.3 μm on ophthalmic imaging at 1.1 μm central wavelength generated from a microstructure fibre pumped by a self mode-locked Ti:sapphire laser [10]. Although excellent for performing ultra high resolution, supercontinuum generation suffers from non-Gaussian spectral shapes and large intensity noise, both factors leading to degradation of the overall OCT system performance.

2. METHOD

Our approach in generating broadband spectrum at 1050 nm is based on superfluorescence from Ytterbium (Yb)-doped and Neodymium (Nd)-doped silica fibres pumped by commercial diode lasers [11]. Yb-doped silica fibres have a broad emission spectrum spanning from 1 μm to 1.15 μm when optically pumping around 980 nm, which makes it an excellent candidate for OCT applications. However, when designing the source configuration, care should be taken, because the achieved bandwidth of an ASE source is usually different from the range in which the spontaneous emission and amplification is observed. Moreover, a desired output spectrum (i.e Gaussian) is only achievable by means of some kind of spectral shaping. This spectral tailoring would ideally be achieved in all-fibre technology conferring a maximum mechanical stability to the complete device.

One challenge in designing a fiber based broadband source is to extract large ASE powers while avoiding laser oscillations. Lasing can occur due to optical feedback from component reflections and/or from Rayleigh backscattering. High isolation is required of single or double stage fiber optical isolators used and low backreflection from all components and splices must be assured. Moreover, larger ASE power densities can be reached before onset of lasing when a Faraday rotator mirror (FRM) is used on the feedback reflection [12]. Another important issue that needs to be addressed is the degree of inversion which influences the spectral shape through interplay between emission and absorption for Yb-doped fibre in the 1050 nm spectral range.

Figure 1a illustrates an Yb-doped fiber ASE source. A 5 m length of Yb-doped fiber is pumped at 975.5 nm through a thin-film WDM 980/1030nm fibre pigtailed coupler. Figure 1b shows the output spectra at the FC/APC connector obtained for different pump power level, P_{pump}. The spectra were measured with an optical spectrum analyzer (OSA, Ando AQ6135A) and the average output optical power with a power meter (Agilent HP 81525A). The effect of the flattening filter on the forward ASE seeding is clearly visible when the pump power is increased.

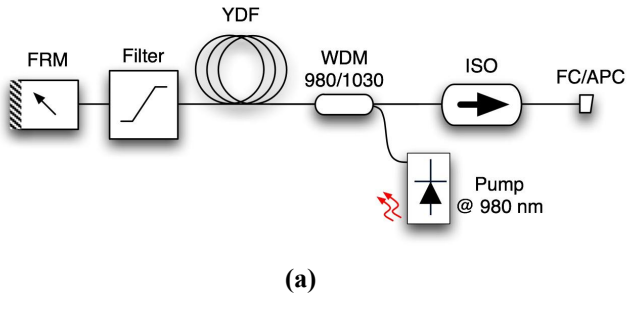

(a)

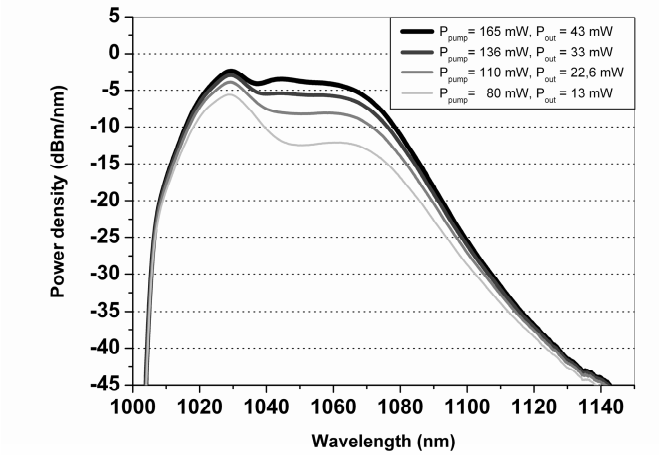

(b)

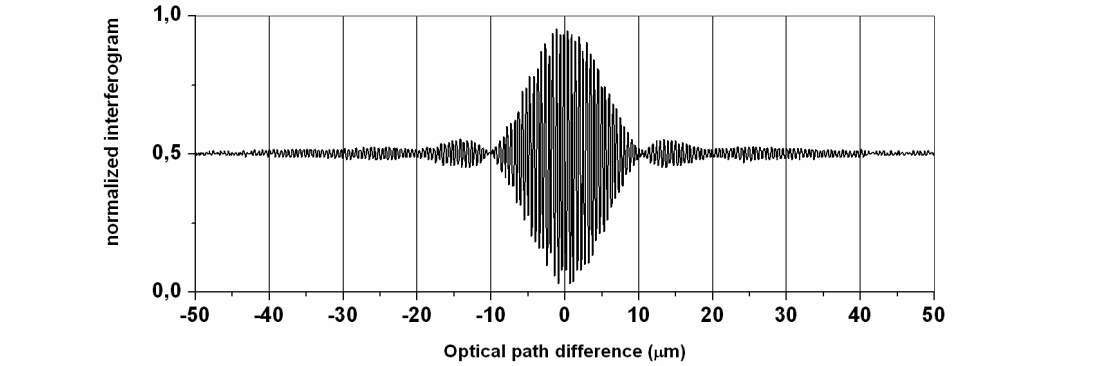

(c)

Figure 1. **(a)** Experimental setup of an Ytterbium ASE source with filtered forward ASE seeding. Faraday rotator mirror (FRM), 975.5 nm pump laser diode (Pump), wavelength division multiplexer fiber coupler (WDM), Ytterbium doped fiber (YDF), optical isolator (ISO), fibre connector angle polished contact (FC/APC). **(b)** Output spectra of the source, for different pump levels. **(c)** Normalized interferogram of the source after spectrum optimization (P_{pump}= 165 mW, P_{out}=43 mW).

The autocorrelation function of the source has been measured using a Michelson interferometer wavelength meter (HP 8612B) modified to give access for measurement of the two detector signals on an oscilloscope. One detector signal gives the reference from a known, stabilized laser source to calibrate the interferometer's mirror movement accurately. The other detector measures the optical interferogram of the source under test. The Yb ASE source interferogram displayed in Figure 1c has a coherence length of 20 µm (defined as FWHM and using a Gaussian fitting function). The magnitude of the side lobes or secondary peaks is less than 10 % of the main peak. In a fully dispersion compensated OCT system the maximum achievable axial resolution is half the coherence length of the source, meaning 10 µm (in air) or ~7 µm in biological samples with the source in fig. 1.

To improve the resolution a broader spectrum is needed; this can be obtained by combining broadband sources with different centre wavelengths to obtain a cumulative broad emission spectrum. Compound broadband superfluorescent fiber sources based on different combinations of rare-earth doped fibres [13-15], or semiconductor optical amplifiers and doped fibre [16], and SLD-based combined light sources [17] have been developed and implemented for OCT systems mostly at 0.8 and 1.5 µm.

A good candidate for broadening the spectrum of Ytterbium, especially towards longer wavelengths range, is Nd-doped fiber. Nd-doped silica-based fibers have been used to demonstrate both single and double-pass ASE operating on the $^4F_{3/2} \rightarrow {}^4I_{11/2}$ transition at 1060 nm with a relative broad emission [18]. We tested two different Nd-doped alumino-germano-phospho-silicate fibers having different Nd^{3+} ion concentration of 1400 ppm and 500 ppm, respectively, pumped by a laser diode at 798.8 nm with ~100 mW maximum power. Both fibers have a 5 μm core diameter, 0.14 numerical aperture (NA) and are optimized in length for a 60dB absorption of the pump power. The higher doped fiber showed very low emission efficiency in the order of hundreds of microwatts for 100mW pump power, even after fiber length optimization. Phenomena like concentration quenching or excited state absorption (ESA) are very likely to occur, being subject also to the glass composition and more pronounced for high doping concentrations [19]. The second Nd-doped fiber sample 500 ppm concentration showed a higher optical efficiency. In single-pass backward pumping configuration ASE power of 4.3 mW was measured. The same fiber used in a double-pass backward pumping configuration as shown in Figure 2a gave even more useful ASE power. This source emitted 15.9 mW with 107 mW of absorbed pump power. The emission spectrum peaking at 1060 nm is asymmetric and the spectral width is independent of pump power. No spurious lasing was observed at maximum available pump power with a gold mirror as optical feedback.

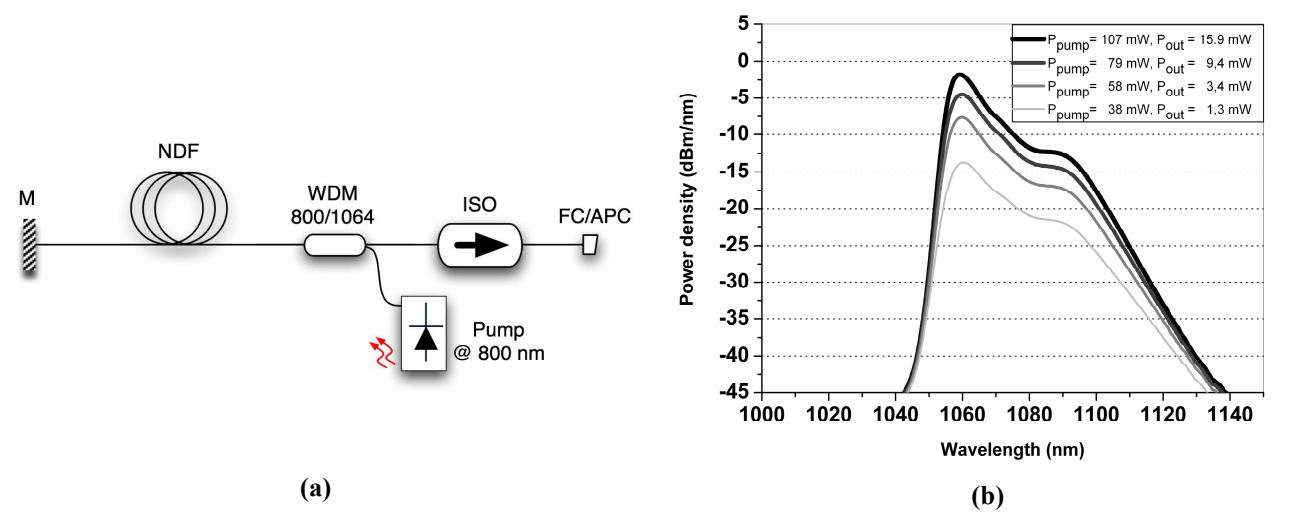

Figure 2. (a) Experimental setup of a Neodymium ASE source with no ASE filtering. Gold mirror (M), 800 nm pump laser diode (Pump), wavelength division multiplexer fiber coupler (WDM), Nd-doped fiber (NDF), optical isolator (ISO), fiber connector angle polished contact (FC/APC). **(b)** Output spectra of the source, for different pump levels.

Comparing Figures 1b and 2b it is noted the Nd has significant emission beyond 1070 nm where the Yb emission drops off. A combination of the emission spectra from the two fibers has the potential of increasing the spectral width.

2.1 Configuration I: Combination of Yb- and Nd-doped fiber emission spectra using a broadband fiber coupler

The first approach used to achieve a broader emitted spectrum was by spectrally adding the Yb- and Nd-doped sources previously discussed in a broadband fibre coupler. We have used a 30:70 splitting ratio fibre coupler as shown in Figure 3a.

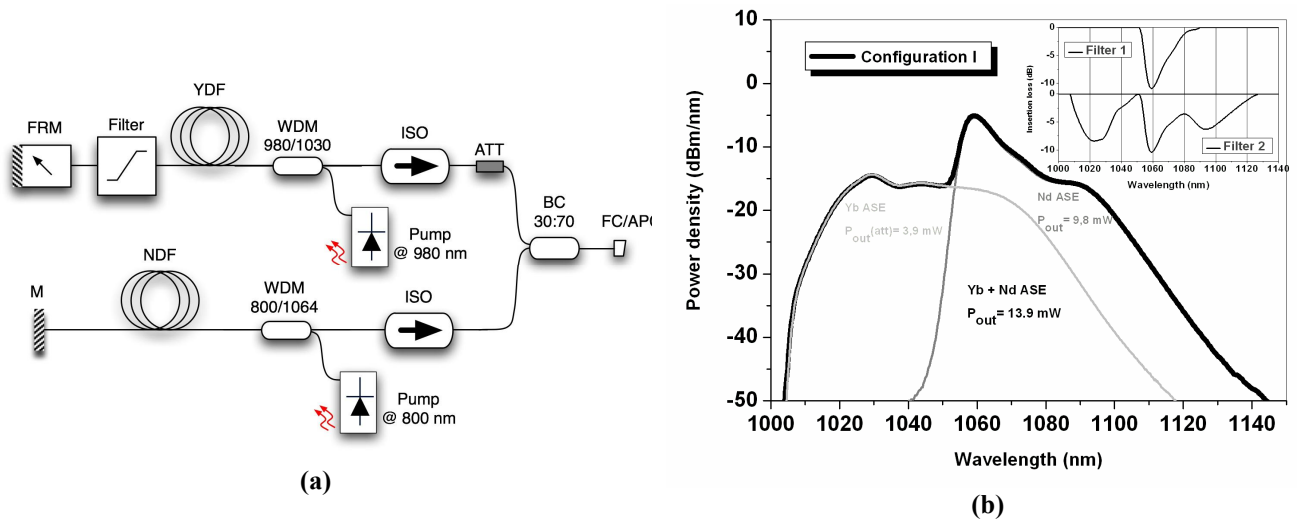

Figure 3. (a) Configuration I for a broadband ASE source with both Yb and Nd emission spectra combined via a broadband fiber coupler (BC), optical attenuator (ATT). **(b)** Measured spectrum for configuration I. The inset box: computer simulated gain-flattening filters: Filter 1 for a flat top spectrum and Filter 2 for a Gaussian spectrum.

The measured output spectra displayed in figure 3b indicate that significant spectrum bandwidth enlargement towards longer wavelengths (~20 nm, at -10 dB level) could be achieved with medium output power, ~ 13.9 mW. The spectral shape can be manipulated using passive filters. In-fibre filter solutions like tilted fiber Bragg gratings (T-FBG) or long period gratings (LPG) could provide such filtering with low excess loss. Thin film filters (TFF) in fiber pigtailed or free space configuration can also be developed to reshape the spectrum. Spectral shaping with passive filters will obviously be at the expense of useful power. The output power could be further increased by an appropriate choice of coupling splitting ratio of the BC. In the present configuration, with the 30:70 splitting ratio fiber coupler, a variable optical attenuator was inserted after Yb-doped ASE source to optimize the output spectrum. Taking into consideration the present configuration's power budget before the coupler and considering the possible optical losses induced by filtering, a 10:90 splitting ratio fiber coupler could prove to be a more appropriate choice.

We are currently investigating different possibilities of spectral shaping the spectrum emitted by this source configuration. We computer simulated the spectral shape of the tailored optical filter for different output spectra. The inset of Figure 3b shows the simulated transmission spectrum required for such filters: (1) for flat top output spectrum and (2) for a Gaussian spectrum. The most straightforward would be a flat-top spectrum shape, with less than 1 dB ripple, which will give more than 70 nm bandwidth at -3 dB with ~ 6 mW output.

Ideally, the spectrum should have a Gaussian shape that will exhibit no secondary peaks in the autocorrelation function of the OCT signal. However, given a flat top shape after filtering and the degree of freedom over parameters like pump power and splitting coupling ratio, the spectrum could be furthermore improved. For OCT applications, both spectral shapes could prove to be beneficiary: Gaussian for a high resolution ASE source; flat top for high resolution swept source.

2.2 Configuration II: Neodymium Amplification by Ytterbium Optical Amplifier

Another approach that we have tested was the combination of two or more concatenated optical amplification stages where the low power output of the first stage is optically amplified by the second stage. Due to the low efficiency and relative narrow emission of the Nd-doped fibre at maximum available pump power, the configurations displayed in

Figures 4a and 4b have been devised for amplifying Nd-doped stage. This approach has been tested with the purpose of extending the Yb ASE spectrum alone without the need of any filtering device. The different spectra shown below have been optimized in terms of spectrum shape and/or output power. The wavelength range to be amplified is different from the range of the ASE emitted by Yb, therefore little or no absorption occurs at these wavelengths; the gain is in the order of ~30 dB. Single stage isolators are used to prevent the source from lasing.

Nd ASE could be seeded either in a forward (Figure 4a) or backward (Figure 4b) optical Yb amplifier configuration. Figure 4c shows a comparison of the output spectra for the two BBS designs. Each plot contains individual spectra obtained for each fiber in each configuration and also the output amplified spectra for a certain set of pump values. The pump parameters for configuration II (a) were: $P_{pump@800}$ = 15 mW and $P_{pump@980}$= 180 mW that gave an output power of about 15.3 mW. For configuration II (b) with $P_{pump@800}$ = 22 mW and $P_{pump@980}$= 150 mW a higher output power of 36 mW was obtained. Compared to the unfiltered Yb ASE spectrum alone shown for comparison (marked as Yb only in the figure 4c) when only Pump@980nm was powered, this approach extends the maximum achievable bandwidth in the long wavelengths region from ~1050 nm to 1070 nm at -5 dB level. However, compared to the previous mentioned backward filtered Yb ASE source (figure 1b) no significant broadening is achieved and the spectral ripples are higher, exceeding -5dB level. In the forward pumping configuration the pit generated by amplifying Nd spectra is smoother than in the backward pumping configuration. However, in terms of optical output power, the backward pumping scheme allows for higher values even with a lower Pump@980nm power and bandwidth extension towards shorter wavelength region. The spectra shown below have been selected to illustrate the effect of Yb amplification on Nd emission. The differences are only due to the Yb ASE spectrum in either backward or forward configuration. Even with pump power optimization, the spectral shape is far away from Gaussian. Moreover, the measured autocorrelation functions (not shown) exhibit high secondary peaks (more than 50 % of the main peak) and therefore cannot be fitted with Gaussian functions anymore.

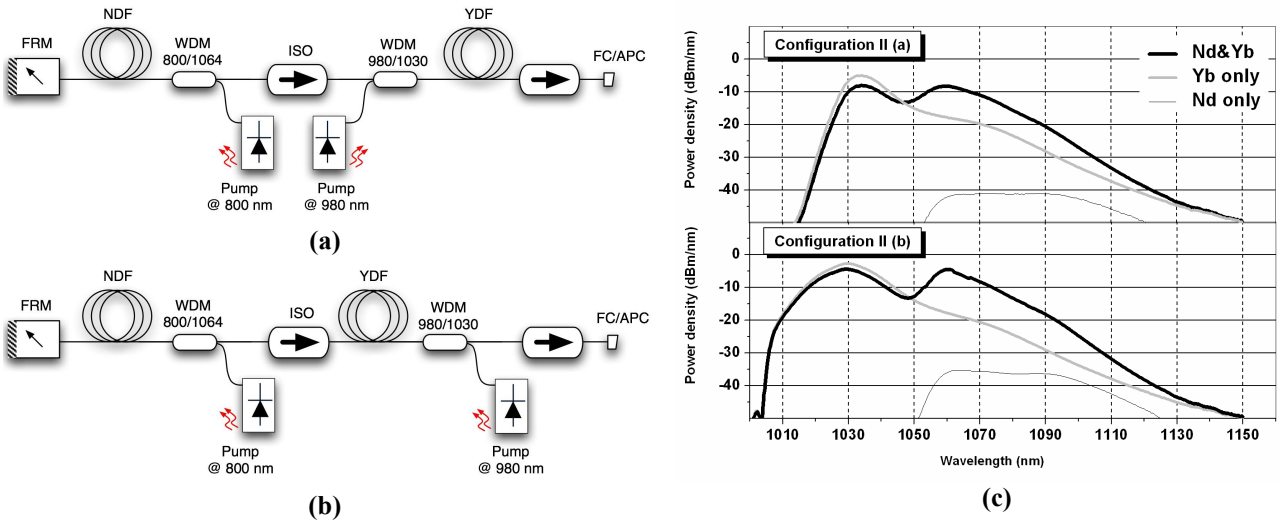

Figure 4. Configuration II of the BBS based on amplification of the Nd output in a forward **(a)** and backward **(b)** optical Yb amplifier. **(c)** Measured output spectra.

A similar configuration with both pumps included and powered simultaneously (Configuration II (2 pumps)) can be operated to provide either broad bandwidth (~70 nm) or high power (70 mW). The best combinations we found in terms of bandwidth or output power while optimizing the pump powers are displayed in figure 5 and their autocorrelation functions compared. The high power output spectrum referred to as (1) in figure 5a exhibits high ripples (> 7 dB) with 40 nm bandwidth at maximum pump power levels. The optimization performed in this case was to bring the two

emission peaks at the same level. The pump parameters are: $P_{pump@800}$ = 18 mW, $P_{pump@980}$= 143 mW (forward pumping) and $P_{pump@980}$= 165 mW (backward pumping). In terms of broad bandwidth output, (2) in figure 5a, the parameters found suitable for a 70 nm bandwidth with less than 2 dB ripples are: $P_{pump@800}$ = 2.4 mW, $P_{pump@980}$ (forward pumping) was under the threshold level and $P_{pump@980}$= 13 mW (backward pumping); only backward pumping was actually performed. However the configuration is unsuitable for practical applications due to very low emission power of about 90 µW. The autocorrelation functions of the two spectra have been measured and compared in figure 5b. Both exhibit side lobes, less visible for the broadband optimized spectrum. The coherence lengths are about 20 µm and 13 µm, respectively.

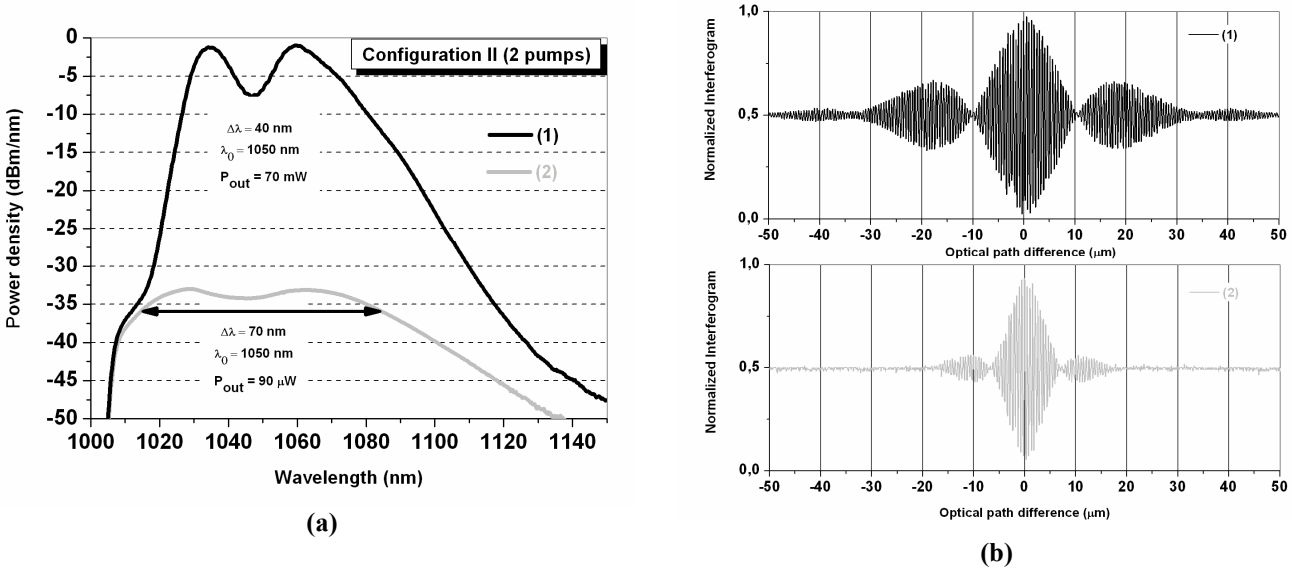

Figure 5. (a) Output spectrum for configuration II with optimized pump power for high power **(1)** and broad bandwidth **(2). (b)** Measured autocorrelation functions of the two spectra.

The same solution as for configuration I could be also employed for Configuration II (either with 1 or 2 pumps), namely filtering. Smoothing the output spectral shape can be preformed using the same approaches: either fiber Bragg gratings or a fiber that will selectively absorb in a specific region of the spectrum. The filter will allow for further increase of the pump level and therefore higher output attainable power and improved bandwidth. Nevertheless it has to be robust, stable, and reliable for building a compact, simple, low cost and efficient broadband source.

3. CONCLUSIONS

Several source configurations based on amplified spontaneous emission of Yb-doped optical fibre have been devised. Their performances in terms of optical power, bandwidth and spectral shape have been tested in order to find the best solution that will meet the necessary requirements for integration in an OCT imaging system with applications in ophthalmology.

Although it is generally accepted that the ideal spectral shape for an OCT system is Gaussian, the spectral shape of most reported broadband sources has been far from Gaussian. These side lobes in the OCT axial response causes actually coherent artefacts in the image. Several approaches have already been employed to minimize these unwanted effects, namely: passive filtering (after the source) and/or post-processing of the coherence function (after registration of the full interferogram). The last solution works well, but still remains problematic for real-time operation. A study on the

maximum permissible value of side lobes could have a great significance in the interpretation and early assessment of different retinal and choroids pathologies, and this is no doubt dependent upon the specific target and purpose.

AKNOWLEDGEMENTS

Irina Trifanov acknowledges the PhD grant from Marie Curie training site supported by the European Commission under the project HIRESOMI (project: Marie Curie EC MEST-CT-2005-020353).

REFERENCES

[1] W. Drexler, J. Fujimoto, "State-of-the-art retinal optical coherence tomography", *Progress in Retinal and Eye Research* **27,** 45–88 (2008).
[2] W. Drexler, U. Morgner, R. K. Ghanta, F. X. Kartner, J. S. Schuman, and J. G. Fujimoto, "Ultrahigh-resolution ophthalmic optical coherence tomography", *Nat. Med.* **7**(4), 502–507 (2001).
[3] A. Unterhuber, B. Považay, B. Hermann , H. Sattmann, A. Chavez-Pirson, and W. Drexler, "In vivo retinal optical coherence tomography at 1040 nm-enhanced penetration into the choroids", *Optics Express* **13**(9), 3252-3258 (2005).
[4] A. N. S. Institute, "Safe use of lasers," ANSI Z136.1–2000, American National Standards Institute, p. 173 (2000).
[5] F. D. Nielsen, L. Thrane, K. Hsu , A. Bjarklev, and P. E. Andersen, "Semiconductor optical amplifier based swept wavelength source at 1060 nm using a scanning Fabry–Perot filter and anYDFA-based booster amplifier", *Optics Communications* **271**, 197-202 (2007).
[6] R. Huber, D. C. Adler, V. J. Srinivasan, and J. G. Fujimoto, "Fourier domain mode locking at 1050 nm for ultra-high-speed optical coherence tomography of the human retina at 236,000 axial scans per second", *Optics Letters* ,**32**(14), 2049-2051 (2007).
[7] E. C. W. Lee, J. F. de Boer, M. Mujat, H. Lim, and S. H. Yun, "In vivo optical frequency domain imaging of human retina and choroid", *Optics Express* **14**(10), 4403-4411 (2006).
[8] B. Považay, B. Hermann, A. Unterhuber, B. Hofer, H. Sattmann, F. Zeiler, J. E. Morgan, C. Falkner-Radler, C. Glittenberg, S. Binder, and W. Drexler, "Three-dimensional optical coherence tomography at 1050 nm versus 800 nm in retinal pathologies: enhanced performance and choroidal penetration in cataract patients", *Journal of Biomedical Optics* **12**(4), 041211-(1-7) (2007).
[9] Y. Yasuno, Y. Hong, S. Makita, M. Yamanari, M. Akiba, M Miura, and T. Yatagai, "In vivo high-contrast imaging of deep posterior eye by 1-μm swept source optical coherence tomography and scattering optical coherence angiography", *Optics Express* **15**(10), 6121-6139 (2007).
[10] Y. Wang, J. Nelson, Z. Chen, B. Reiser, R. Chuck, R. Windeler, "Optimal wavelength for ultrahigh-resolution optical coherence tomography", *Optics Express* **11**(12), 1411-1417 (2003).
[11] R. Paschotta, J. Nilson, A. Tropper, D. Hanna, "Ytterbium-Doped Fiber Amplifiers", *IEEE Journal of Quantum Electronics*, **33**(7), 1049-1056 (1997).
[12] J. M. Sousa, M. Melo, L. A. Ferreira, J. R. Salcedo, and M. O. Berendt, "Product design issues relating to rare-earth doped fiber ring lasers and superfluorescence sources", in Proc. SPIE vol. **6102**, Fiber lasers III: technology, systems, and applications (23-26 January 2006, San Jose, California, USA) pp. 610223.1-610223.12 (2006).
[13] H. Chen and G. W. Schinn, "Hybrid broadband superfluorescent fiber source consisting of both thulium-doped fiber and erbium-doped fiber", *Optics Communications* **229,** 141–146 (2004).
[14] R. Paschotta, J. Nilsson, A. Tropper, and D. Hanna, "Efficient superfluorescent light sources with broad Bandwidth", *IEEE Journal of Selected Topics in Quantum Electronics*, **3**(4), 1097-1099 (1997).
[15] K. Haroud, E. Rochat, and R. Dändlicker, "A broad-band Superfluorescent fiber laser using single-mode doped silica fiber combinations", *IEEE Journal of Quantum Electronics*, **36**(2), 151-154 (2000).

[16] D. Beitel, L.Carrion, L. R. Chen, and R. Maciejko, "Development of Broadband Sources Based on Semiconductor Optical Amplifiers and Erbium-Doped Fiber Amplifiers for Optical Coherence Tomography", *IEEE Journal of Selected Topics in Quantum Electronics*, **14**(1), 243-250 (2008).
[17] E. V. Andreeva, P .I. Lapin, V.V. Prokhorov, V. R. Shidlovski, M. V. Shramenko, and S.D. Yakubovich, "Novel Superluminescent Diodes and SLD-based Light Sources for Optical Coherence Tomography", in Proc. of SPIE-OSA Biomedical Optics, Optical Coherence Tomography and Coherence Techniques III, vol. 662 7662703 (2007).
[18] M. J. F. Digonnet, K. Liu, "Analysis of a 1060-nm Nd:SiO2 superfluorescent fiber laser", *J. Lightwave Technol. 7*, 1009-1015 (1989).
[19] Y. Qiao, N. Da, D. Chen, Q. Zhou, J. Qiu, and T. Akai, "Spectroscopic properties of neodymium doped high silica glass and aluminum codoping effects on the enhancement of fluorescence emission", *Appl. Phys. B* **87**, 717–722 (2007).